

Issues in joint SZ and optical cluster finding

J.D. Cohn¹ and Martin White²

¹*Space Sciences Laboratory,*

²*Departments of Physics and Astronomy,
University of California, Berkeley, CA 94720*

5 November 2018

ABSTRACT

We apply simple optical and SZ cluster finders to mock galaxy catalogues and SZ flux maps created from dark matter halos in a $(1 h^{-1}\text{Gpc})^3$ dark matter simulation, at redshifts 0.5 and 0.9. At each redshift, the two catalogues are then combined to assess how well they can improve each other, and compared to several variants of catalogues made using SZ flux and galaxy information simultaneously. We use several different criteria to compare the catalogues, and illustrate some of the tradeoffs which arise in tuning the galaxy cluster finders with respect to these criteria. We detail many of the resulting improvements and issues which arise in comparing and combining these two types of data sets.

1 INTRODUCTION

In order to study galaxy clusters one must first find, and ideally weigh, them. Catalogues spanning a range of redshifts, with a well understood selection function, are key to learning about many cluster properties – for a recent review, see e.g. Voit (2005). These include counting clusters as a function of redshift to study dark energy and cosmological parameters, characterizing them as environments for galaxy formation, and for understanding galaxy cluster formation and evolution itself. As galaxy clusters correspond to the largest dark matter halos in numerical simulations, many of the statistical properties of the galaxy cluster population are theoretically accessible. Indeed, predictions for dark matter halo properties in collisionless N-body simulations are converging (Evrard et al 2008; Heitmann et al 2008; Lukic et al 2008; Tinker et al 2008). The number and positions of cluster sized halos (their counts and clustering) are of interest for dark energy applications, while for cluster and galaxy properties and evolution these halos comprise the backbone for the more complex and less well understood cluster and galaxy gas physics.

In this note we study mock cluster samples produced by finding overdensities of galaxies or distortions in the cosmic microwave background produced by the up-scattering of CMB photons by the hot intra-cluster gas (Sunyaev & Zel’dovich 1972, 1980, hereafter SZ). We compare catalogues found from both methods optimized separately, optimized as a pair, and using one catalogue as input for the second catalogue’s search algorithm – a first attempt at joint optical-SZ cluster finding. We identify trends in the resulting samples, as well as new issues and tradeoffs which arise once SZ and optical data are jointly available. The general features we find can be expected to have bearing on surveys using optical and SZ cluster finding together, such

as the (optical) Dark Energy Survey (DES¹) and the (SZ) South Pole Telescope (SPT²) experiment.

The advantage of combining two cluster finding methods is that each method has different strengths and weaknesses. For example, SZ cluster finders can successfully find high mass halos (e.g. $\geq 2 \times 10^{14} h^{-1} M_{\odot}$) but do not give accurate redshifts³, while optical cluster finders can miscast a low mass halo as a high mass one, but are much better at obtaining redshifts (albeit still with possible errors). Both optical and SZ cluster finders suffer from projection effects but possibly in different ways as they trace different properties of the baryonic matter. (Projection has been an issue for optical cluster finding since the earliest surveys, e.g. Abell (1958); Dalton et al (1992); Lumsden et al (1992); White et al (1999), and has been estimated in SZ by White, Hernquist & Springel (2002); Holder, McCarthy & Babul (2007); Hallman et al (2007); Shaw, Holder & Bode (2007).) As the largest objects which have had time to virialize in the universe, “average” cluster properties evolve with redshift, and so the results of joining SZ and optical may evolve as well.

The outline of our paper is as follows. We start by describing the simulations and (standard) catalogue/map constructions in §2. In section §3 we describe the (again standard) optical and SZ cluster finders separately, and the resulting catalogues. As our interest is in general properties, we restrict ourselves to relatively simple cluster finders. Along with the finders, criteria for assessing the success of a finder are introduced and applied to a fiducial optical catalogue, for comparison with the catalogues produced with the other finders in the rest of the paper. In §4, we compare the

¹ <http://www.darkenergysurvey.org>

² <http://pole.uchicago.edu>

³ Though rough estimates are possible using SZ morphology (Schaefer, Pfrommer & Zaroubi 2005).

optical and SZ cluster catalogues to the dark matter halo catalogues, and then introduce a matching between the optical and SZ catalogues directly. We measure how each catalogue is improved by the additional information from the other. Since the matching is not always one-to-one (one optical cluster to one SZ cluster), the augmented SZ catalogue (with optical information) has different information than the improved optical catalogue (with SZ information). Lastly, a joint finder based on optical galaxies and SZ flux is introduced, and two other steps in complexity are added, and these cases are compared to the previously discussed ones.

We identify the trends in all of these catalogues as a function of finder methods and parameters using our success criteria. More detail about redshift success (a crucial use of the optical catalogue and/or galaxies for SZ) and whether the SZ and optical information can be combined to veto outliers are found in §5. §6 summarizes, discussing the many improvements due to combining the finders, trends which are expected to generalize beyond our simple finders and catalogues, and issues which have been raised.

2 SIMULATIONS: DARK MATTER, GALAXY CATALOGUES AND SZ MAPS

N-body simulations provide a means of making mock catalogues with halos situated in their correct cosmological context, capturing the population properties, their environmental dependences, and projection effects. We use a 1024^3 particle dark matter simulation in a periodic box of side $1 h^{-1}\text{Gpc}$ run with the TreePM code described in White (2002). This code compares well with others in code comparison tests (e.g. Heitmann et al 2008; Evrard et al 2008). The cosmological parameters, $\Omega_m = 0.25$, $\Omega_\Lambda = 0.75$, $h = 0.72$, $\Omega_B h^2 = 0.0224$, $n = 0.97$ and $\sigma_8 = 0.8$, are in accord with a wide array of cosmological observations. The particle mass is $6 \times 10^{11} h^{-1} M_\odot$ and the force softening length is $35 h^{-1}\text{kpc}$, allowing us to easily resolve the halos of interest. Further details of the specific simulation can be found in Brown et al. (2008). We use fixed time outputs at $z = 0.5$ and $z = 0.9$ and make use of the periodicity of the simulation volume to avoid issues concerning boundary effects in the maps or catalogs (otherwise the boxes would span about 0.4 (0.6) at $z = 0.5(0.9)$ in redshift). Periodicity allows objects in any part of the box to be subject to analogous projection effects.

For each output we identify dark matter halos in three dimensions using the Friends-of-Friends (Davis et al. 1985) algorithm, with linking length 0.168 times the mean interparticle spacing⁴. This is slightly smaller than the oft used 0.2 linking length. We found that the longer linking length could over-merge halos; with our choice we only link two regions if the density in the bridge connecting them is $> 100 \rho_b$ everywhere. We shall use these FoF masses throughout.

At $z = 0.5$ there are 7173 (1516) halos with $M \geq 1(2) \times 10^{14} h^{-1} M_\odot$, compared with 2167 (295) at $z = 0.9$. These halos will be the sought after objects in our cluster searches. The observables (red galaxies and SZ flux) of the

halos are added to the simulation in post processing as described below.

2.1 Red Galaxy Mock catalogues

Observationally cluster galaxies are predominantly red, with little or no on-going star formation. Most clusters at low z are observed to have a tight ‘‘red sequence’’, and overdensities of galaxies in this sequence can be used to find clusters (Bower, Lucey, & Ellis 1992; Lopez-Cruz 1997; Gladders & Yee 2000; Lopez-Cruz, Barkhouse & Yee 2004; Gal, Lubin & Squires 2005; Gladders & Yee 2005; Gladders et al 2006; Wilson et al 2006). In order to mimic these galaxies, we populate the halos in our simulation with red galaxies in a manner which reproduces the luminosity function and luminosity dependent clustering seen in the NDWFS (Jannuzi & Dey 1999), as modeled in White et al (2007) and Brown et al. (2008), over a range of redshifts. The clustering of our model galaxies is remarkably consistent with that found subsequently for 2SLAQ (Ross et al. 2007, Ross, private communication).

We model photometric redshift errors for these (red) galaxies as a Gaussian of width $\delta z = 0.02(1+z)$. (We explored trends with larger and smaller photometric errors, which degraded or improved the finders as expected.) We did not include a population of objects with ‘catastrophic’ redshift failures, or a population of blue galaxies for which photometric redshifts are generally less accurate. Models of these objects are less well developed. As we will see below, the optical cluster finding was difficult enough without adding these complications and we wanted to focus on the main features of the method rather than the details which would need to be addressed by a finder operating on observational data.

We assumed that the photo- z errors were uncorrelated for different galaxies within each cluster, unless stated otherwise. If photo- z errors were correlated for galaxies within the same cluster – perhaps due to shared evolution – the observed cluster would shift rather than spread in the redshift direction. We looked at 10 clusters in the SDSS C4 (Miller et al 2005) catalogue lying in the equatorial stripe in the range $0.07 < z < 0.15$, for which both spectroscopic and photometric redshifts of the member galaxies are known. For these it appears that the photometric redshift errors are at most weakly correlated. The upside of this is that the error on the mean redshift of the cluster galaxies is significantly tighter than on an individual galaxy. While we cannot be sure that this decorrelation holds at higher redshift or with different filters, we note that some scatter in photo- z is expected from photometry errors in any case, so we can consider our approach to be conservative for finding clusters.

The resulting mock galaxy catalogues have objects with a 3D position, luminosity and an observed photo- z . We keep all galaxies brighter than $\frac{1}{2}L_*$, giving $\sim 4(3) \times 10^6$ galaxies at redshifts 0.5 (0.9).

2.2 SZ flux maps

The dark matter simulations are also used to create SZ y -distortion maps for both redshifts, using the method described in detail in Schulz & White (2003) and

⁴ This defines halos to be the material above a density threshold of roughly $\rho > 3/(2\pi b^3) \simeq 100$ times the background density, with no requirement on the halo shape.

Vale & White (2006). To recap briefly, the gas is assumed to follow the dark matter density and to be at a uniform temperature $T \propto M^{2/3}$, with a low- M cut-off for halos below 1 keV. The y -distortion is computed by projecting through the material in the box, using the non-relativistic expression (Sunyaev & Zel'dovich 1972, 1980). These approximations are poor in detail, and can be easily improved upon, but provide a good approximation to more realistic y maps produced by hydrodynamic simulations (e.g. White, Hernquist & Springel 2002) when smoothed with the $1'$ beam of upcoming experiments (e.g. SPT). Such a beam subtends $400 h^{-1} \text{kpc}$ at $z = 0.5$ and $600 h^{-1} \text{kpc}$ at $z = 0.9$, making the maps largely insensitive to the detailed cluster physics and to our N-body resolution. Our cluster finding, described below, also uses the integrated flux across the whole peak, as this is expected to be a more robust measure of cluster mass. This approach down-weights the omitted effects even more. We note however that by assigning T given the halo's mass, and ignoring its dynamical state, we are likely underestimating the scatter in the $Y - M$ relation.

Assuming the distant observer, or plane parallel, approximation, a map for each redshift of 4096^2 pixels is created by projecting through the $1 h^{-1} \text{Gpc}$ length of the box. As for the galaxy catalogs, the resulting maps are periodic, allowing us to ignore edge effects below. The pixels subtend $0.6'$ at $z = 0.5$ and $0.4'$ at $z = 0.9$, comfortably below the $1'$ instrument beam we shall assume below. We converted from Compton y -parameter to temperature distortion assuming an observing frequency of $\nu/56.84 \text{ GHz} \ll 1$, though this choice is degenerate with our assumed normalization of the $T - M$ relation. The overall normalizations of the maps was set by comparing T and Y as a function of halo mass in the simulation to the similar correlations observed in X-ray by Arnaud, Pointecouteau & Pratt (2007).

The resulting maps were smoothed with a Gaussian of width $1'$, to approximate the instrumental response, and gaussian noise of $20 \mu\text{K-arcmin}$ was added. The resolution and noise were chosen to be similar to that expected for SPT (Ruhl et al 2004). This is a best case estimate, as it ignores issues of CMB cleaning, foreground contamination or systematics. In order to increase contrast of the peaks in our maps, we smoothed it once again by a Gaussian of width $1'$ and it is these maps which we used for our cluster finding.

3 OPTICAL AND SZ CLUSTER FINDING

We start by constructing separate optical and SZ cluster catalogues, such as two separate surveys might produce, using simple finders to focus on general trends. We will call the found objects ‘‘clusters’’, while the true objects in the underlying dark matter catalogue will be called ‘‘halos’’. Our main focus will be on ‘‘massive halos’’, by which we mean those with $M \geq 2 \times 10^{14} h^{-1} M_{\odot}$. Massive halos in our cosmology have $\bar{n} \simeq 1.6 \times 10^{-6} (h^{-1} \text{Mpc})^{-3}$ and $\sim 2.8 \times 10^{-7} (h^{-1} \text{Mpc})^{-3}$ at $z = 0.5$ and 0.9 respectively.

3.1 Optical Finder

Our optical finder is a refinement of the circular overdensity method used in Cohn et al (2007). The galaxies are first sorted by luminosity. Starting with the most luminous each

galaxy is considered in turn as a potential cluster center. Every other galaxy is given a weight dependent upon the galaxy's estimated position from the candidate cluster center,

$$g(\delta r_3) = \exp \left[-\frac{1}{18} \left(\frac{|\delta r_3|}{\sigma} \right)^3 \right] \quad (1)$$

where σ is the photometric redshift error, expressed in $h^{-1} \text{Mpc}$, and δr_3 is the distance from the central galaxy in the redshift direction. This weight g is multiplied by a second weight depending upon previous membership in other clusters⁵. If we write r_{clus} for the radius of the found cluster, and r_{\perp} for the radial distance of the galaxy in two dimensions from the cluster center then the second weight for each galaxy starts as unity and is decreased by

$$\Xi(r_{\perp}, \delta r_3) = g(\delta r_3) \left(1 + 16 \frac{r_{\perp}^2}{r_{\text{clus}}^2} \right)^{-1} \quad (2)$$

each time the galaxy is included in a cluster with $g(\delta r_3) > g(3\sigma) \simeq 0.223$. The second weight for a galaxy is set to zero if its value goes negative.

For each candidate center, starting with the 8 galaxies closest to (and including) the center in the plane of the sky, the weights are summed to define an overdensity

$$\Delta \equiv \frac{\sum_i g(\delta r_{3,i}) \Xi(r_{\perp,i}, r_{3,i})}{\pi r^2 \bar{n}_{\text{gal}}} \quad (3)$$

where the index i refers to the i th galaxy, r is the distance to the farthest of the 8 galaxies and \bar{n}_{gal} is the average surface density of galaxies. We calculated \bar{n}_{gal} by taking the average around 1000 randomly chosen galaxies in the simulation. The cluster is kept if $\Delta \geq \Delta_p$, a critical (or threshold) density and a parameter in our finder. For any cluster found, the nearest galaxies are added until $\Delta < \Delta_p$ and all contributing galaxies which have $g(\delta r_3) > g(3\sigma)$ are removed from the list of subsequent potential cluster centers and given a decreased weight $\Xi(r_{\perp}, r_3)$ as described above.

As usual with overdensity finders, choosing a high value of Δ_p picks out the halo cores and misses many halos entirely, while a lower value blends many halos into one cluster. After some experimentation we set Δ_p by measuring its value on $\sim 10^3$ massive halos ($M \geq 2 \times 10^{14} h^{-1} M_{\odot}$) using the radius containing 55% of the halo galaxies. Our fiducial threshold (below) is the 67th percentile of the Δ_p distribution of these objects.

The halo whose galaxies contribute the most to the weighted sum over the cluster galaxies we call the best match halo, and f_{best} is defined to be the best matched halo's fractional contribution to the full cluster's weight⁶ (Another possibility for matching to a halo is to take the halo of the central galaxy in the cluster, the analogue of the BCG. We found that this doesn't work as well using our criteria for success, described below.) The mass of the best matched halo is assigned to the cluster. Clusters with $f_{\text{best}} \geq 0.5$ will

⁵ This means that changing parameters to find different clusters is different than finding a larger cluster sample and then making a cut on the full sample afterwards. Each galaxy contributes to potential clusters based on its membership in previous ones.

⁶ This is analogous to the ‘‘Largest Group Fraction’’ and ‘‘Largest Associated Group’’ used by Gerke et al. (e.g. 2005).

be considered clean, clusters with lower values of f_{best} will be called blends.

We define the cluster’s richness to be the sum of its galaxy weights and we only consider clusters with richness ≥ 10 hereon. The optical cluster finding thus produces a list of halos with the “richest” cluster associated to each and a list of clusters with a richness, a redshift (of the central galaxy), a best matched halo (its mass and three dimensional position) and a measure, f_{best} , of how good of a match this halo is.

3.2 SZ finder

Cluster finding in the SZ flux maps follows Schulz & White (2003). Peaks above $4\sigma_{\text{noise}}$ ($80 \mu\text{K-arcmin}^2$) in the map are identified and clusters are grown around these until all contiguous pixels with flux at least 25% of the maximum are included. In most of the discussion below (unless specified otherwise) adjacent peak regions are merged and assigned to the highest peak. Each patch is then associated with the sum of fluxes from each of its pixels. The flux overdensities are matched to halos with centers within two pixels ($\sim 500 h^{-1}\text{kpc}$) of the patch; the halo with the largest mass is taken to be the best matched halo. Most ($> 95\%$) of the peaks were matched to < 6 halos of mass $> 10^{13} h^{-1} M_{\odot}$, the most matched peak had 18 matches. The number of matches is due to the sky area subtended by each patch (on average about $1 (h^{-1} \text{Mpc})^2$ or ~ 18 pixels) and the lack of line-of-sight information from the SZ map itself. The number of halos per patch is larger than expected based on purely Poisson statistics (given the very low number densities of halos), but the halos exhibit significant clustering, enhancing the number within any given SZ patch.

The resulting SZ cluster catalogue contains the SZ flux and two dimensional peak position for each patch, and the best matched (most massive) halo and its three dimensional position. We also kept the number of pixels in the SZ patch but did not use it in the analysis as it is $\simeq 75\%$ correlated with the total SZ flux in the patch.

4 OPTICAL AND SZ CATALOGUE COMPARISON

We now have three catalogues in hand: the optical cluster catalogue, the SZ cluster catalogue and the halo catalogue (our “truth”). A perfect finder would find every massive halo as a cluster once and only once, with the finder observables richness and flux that are well correlated with its mass and – for the optical catalogue – a correct redshift. However, catalogues can succeed better or worse at different combinations of these properties.

In order to compare the catalogues, we measure the following quantities, which all tend to zero in the ideal case:

- the number of halos with $M \geq 2 \times 10^{14} h^{-1} M_{\odot}$ which are not the best match halo of any cluster (missed)
- the number of blends (clusters with $f_{\text{best}} < 0.5$), for clusters with an optical richness only
- the scatter in the least squares fit to the $\lg(\text{richness})$ - $\lg(\text{mass})$ relation (and $\lg(\text{flux})$ - $\lg(\text{mass})$ when SZ is included),

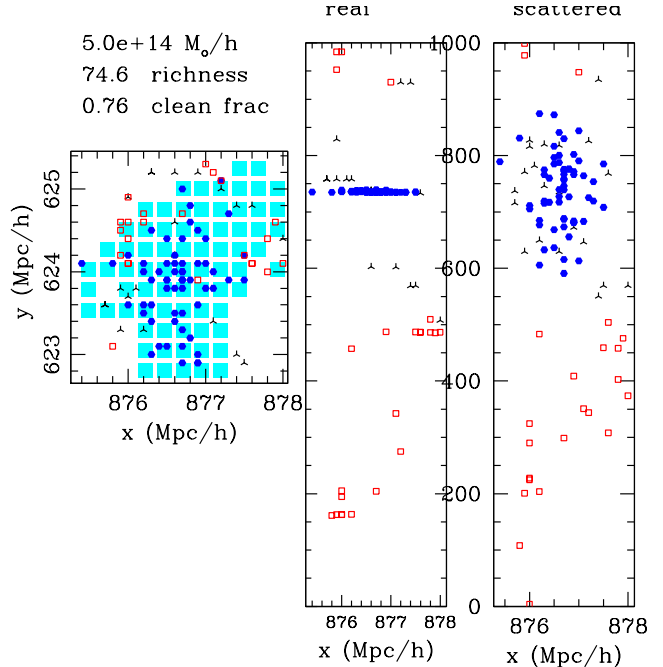


Figure 1. A rich clean cluster. At left is the view on the plane of the sky. The shaded regions are pixels of SZ flux in the corresponding found SZ cluster. The filled circles are galaxies belonging to the halo contributing the most richness to the cluster, the little “T” marks are galaxies not from the dominant halo, but still contributing richness $\geq 1/3$ to the cluster, and the open squares are galaxies who each contribute richness less than $1/3$ (and thus are not really considered part of the cluster). At right, the two long stripes show the position of the galaxies in the x vs. redshift direction. The scale in the redshift (vertical) direction runs the full $1000 h^{-1} \text{Mpc}$ of the box. The true redshift direction positions are shown in the lefthand stripe, and the observed, scattered positions are shown in the righthand stripe. The “puffing out” of the cluster in the redshift direction is clearly visible.

- the number of overcounted massive halos (the number of massive halos found as best match minus the number found as best match which are unique, divided by the total number of massive halos in the box).

In addition, the separation between the measured and true redshift will be measured for finders which provide a redshift.

These criteria are not all independent. Blends, for example, will increase scatter in the richness-mass relation, but also tend to change the shape of the scatter (Cohn et al 2007). The mass distribution for blends, for a given richness cut, is centered around a lower mass than that for the clean clusters. One might want to favor one criterion strongly over another however. For instance, if one is building a catalogue for X-ray followup, rather than measuring the statistical properties of the full halo distribution, one might want to minimize blends to the extreme at the cost of losing many massive halos.

4.1 Optical Cluster results

To illustrate the range of behaviours we see in the simulations, we first present some case studies. Fig. 1 shows a very

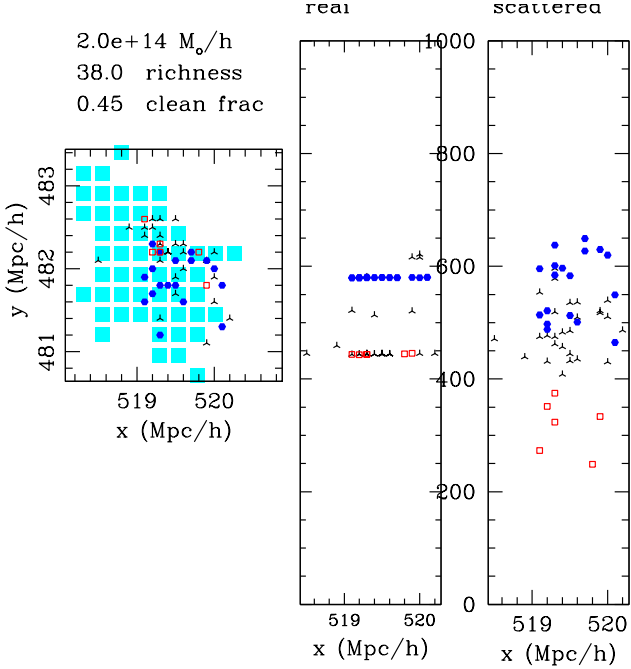


Figure 2. Example of a very rich blended cluster, with points having the same meaning as in the previous figure. Notice how the photo- z errors have “puffed” out the galaxy positions of two halos separated by $> 100 h^{-1}\text{Mpc}$, mixing them up.

rich and massive ($M = 5 \times 10^{14} h^{-1} M_{\odot}$) clean cluster. The effect of photo- z scatter can be clearly seen in the “puffing out” of the galaxies in the redshift direction, but the cluster is still identified by our finder. Fig. 2 shows a more complex example. This blended optical cluster has a $2 \times 10^{14} h^{-1} M_{\odot}$ halo contributing most of its richness, but is blended with another halo of mass $1.4 \times 10^{14} h^{-1} M_{\odot}$ about $150 h^{-1}\text{Mpc}$ away. In general the combination of photo- z scatter and the non-circular halo shape complicates the matching clusters and halos. Halos can also be missed because they are abnormally poor for their mass (the number of satellites in each halo is Poisson distributed) or because they are too close to another halo and get confused with it.

For our fiducial choice of cluster finding parameters the optical catalogue misses $\sim 15\%$ of the massive halos, has 14% blends, a scatter in $\lg(\text{richness})-\lg(\text{mass})$ of 0.30 and the overcounts equal 17% of the total number of massive halos. (To clarify what we mean by overcounts: 264 of the best match halos were already the best match halo at least once.) The $\lg(\text{richness})-\lg(\text{mass})$ relation is shown in Fig. 3. Recall that we require a minimum richness of 10 for a cluster to be included in the optical catalogue. This scatter is large, but note that there is an intrinsic scatter in the $\lg(\# \text{ galaxies})-\lg(\text{mass})$ relation for the halos of $0.13 \lg(\text{mass})^7$. The richness-mass scatter can be reduced slightly by using the sum of cluster galaxy luminosities (for cluster galaxies with $g(\delta r_3) > g(3\sigma)$) as a mass indicator, and more re-

finer measures could possibly improve this further. As in Cohn et al (2007), for a given fixed richness cut the blends seem centered at a lower mass than the clean clusters. The blends thus produce a bimodality in the richness-mass relation. At redshift $z = 0.9$, the catalogue has 14% missed massive halos, 23% blends, 0.34 scatter in $\lg(\text{mass})$ and overcounts equalling 15% of the massive halos in number. The increase in blends with redshift occurred also with the color based finder in Cohn et al (2007).

If instead of using the most contributing halo as the cluster halo, one takes the halo of the central galaxy as the optical cluster halo (“the BCG halo”)⁸, the halo matching changes for 8% of the $z = 0.5$ optical clusters. The number of missed halos goes up as clusters more often get identified with lower mass halos rather than the more massive ones. Not surprisingly, the number of blends goes up as well: if the BCG halo and most contributing halo coincide then the BCG halo is already the fiducial optical cluster halo. A change to any other halo means a change to a halo contributing fewer galaxies and thus a change to a blend. The $\lg(\text{richness})-\lg(\text{mass})$ scatter goes up (because more optical clusters are now matched with low mass halos) and the amount of overcounting goes down slightly (from 17% to 13% of the number of massive halos). This supports the use of the most contributing halo as the best match halo for the optical cluster. What appears to be happening at least some of the time is that a massive halo is “caught” by a luminous galaxy which scatters into its redshift range and becomes its center due to photo- z errors.

Several tunable parameters/functions are part of the optical cluster finding: the minimum density to be labelled a cluster, Δ_p , the minimum number of galaxies to require before imposing the overdensity requirement, the weights in the redshift direction, and downweighting in radial direction. We varied these to try to minimize the number of blends and maximize the number of found massive halos. For example, changing the overdensity Δ_p can decrease the number of blends, the scatter in the richness-mass relation and overcounting, but increases the number of missed halos, and vice versa. We experimented with the weight g in order to catch some of the 32% of cluster galaxies with more than the 1σ photo- z errors, but not to catch too many galaxies too far out.

Smaller observational errors can of course improve the cluster finding. For example, in the extreme limit that the redshift errors are reduced to $10 h^{-1}\text{Mpc}$, if we again use the radius containing 55% of the halo galaxies to calculate Δ_p , Δ_p goes up by a factor of 6, the finder misses 30% more of the massive halos, cuts the blends by 70%, the scatter by 25% and slightly reduces the overcounting.⁹ Lowering Δ_p to miss fewer massive halos than the fiducial case still decreases the blends by 70%, the scatter by 20% and the overcounting (though not by as much). In contrast, increasing the photo- z errors to 5% and changing Δ_p to miss the same number of massive halos as in the fiducial case raises the number of blends by a factor of 2.4.

⁷ The lowest mass halos dominate our counts and have 10 galaxies. Ignoring the central and assuming Poisson statistics (Kochanek et al 2003), we expect $9 \pm \sqrt{9}$ satellites at fixed mass or, since the $N - M$ relation is close to linear, a 30% scatter in M at fixed N . Since $\lg M \simeq 0.4 \ln M$ this is $\delta \lg M \simeq 0.12$.

⁸ We thank A. Leauthaud and R. Nichol for suggesting we quote this number.

⁹ Changing the redshift errors changes the contrast with the background density for the clusters used to calibrate Δ_p .

Another possibility, mentioned above, is that the photo- z errors are correlated within a given halo, due perhaps to similar star formation histories for the member galaxies. As noted we did not see such a trend in the low- z C4 catalog, but if present it would reduce the “puffing out” in the redshift direction and make halos easier to find. In the simulations we experimented with a fully correlated scatter in the redshift direction and saw a strong improvement, as expected. When all photo- z errors are the same for galaxies within the same halo then in comparison to the fiducial case the number missed is slightly smaller, the number of blends drops by almost 50%, the scatter by 10% and the overcounting by about 20%.

The finder also does much better for the $\sigma_8 = 0.9$ catalogues of Cohn et al (2007), which implies a non-trivial dependence upon σ_8 of the finder at fixed mass cut. Essentially, a lower σ_8 is analogous to fixing σ_8 and raising the mass or redshift – increasing the number of disturbed halos, increasing the relative number of possible low mass interlopers for a given high mass halo and decreasing the halos’ contrast with the background more generally. This has been seen in other studies: Lukic et al (e.g. 2008) find that FoF and SO finders differ more at high redshift and lower σ_8 universes. This is very relevant to our situation as we are using an SO cluster finder to search for FoF dark matter halos.

4.2 SZ cluster results

We now turn to the SZ cluster finder, again starting with an example. An example of an SZ cluster is shown in Fig. 4, corresponding to the optical cluster shown earlier in Fig. 1. The SZ cluster is centered on the most massive $5 \times 10^{14} h^{-1} M_\odot$ halo it contains, but also has a $1.4 \times 10^{14} h^{-1} M_\odot$ halo matched to it.

The $\lg(\text{flux})-\lg(\text{mass})$ relation for the SZ cluster catalogue on its own is shown in Fig. 5. More than 98% of the massive halos are found at $z = 0.5$ (and $> 99\%$ at $z = 0.9$), the $\lg(\text{flux})-\lg(\text{mass})$ relation has a scatter of ~ 0.10 in $\lg(\text{mass})$ and the overcounting is slightly smaller than the optical fiducial case (13%). For redshift $z = 0.9$ the scatter is similar and the overcounting is 15%, still smaller than fiducial optical value 17%. We do not apply the blend criterion to the SZ only clusters.

Almost all the massive halos which are missed are inside an SZ cluster, but are not the most massive halo in that SZ cluster. The tight relation between SZ flux and mass is known, and seen as well in our simulations: the scatter in $\lg(\text{flux})-\lg(M)$ is smaller than between $\lg(\text{richness})-\lg(M)$. The scatter in flux in our simulations is caused by projection and is also well known (White, Hernquist & Springel 2002; Holder, McCarthy & Babul 2007; Hallman et al 2007; Shaw, Holder & Bode 2007) – see Holder, McCarthy & Babul (2007) for a calculation of the dependence upon σ_8 . There are, as noted above, approximations in the maps which might cause improvements in the SZ cluster finding. The projection noise in our simulations might be slightly smaller than in reality because we project only through the $1 h^{-1} \text{Gpc}$ box rather than through the full path from $z \sim 10^3$ to $z \simeq 0$. Our maps have also minimized the intrinsic dispersion in the flux–mass relation because we assume a simple functional form for T_{gas} given M , independent of the halo’s history

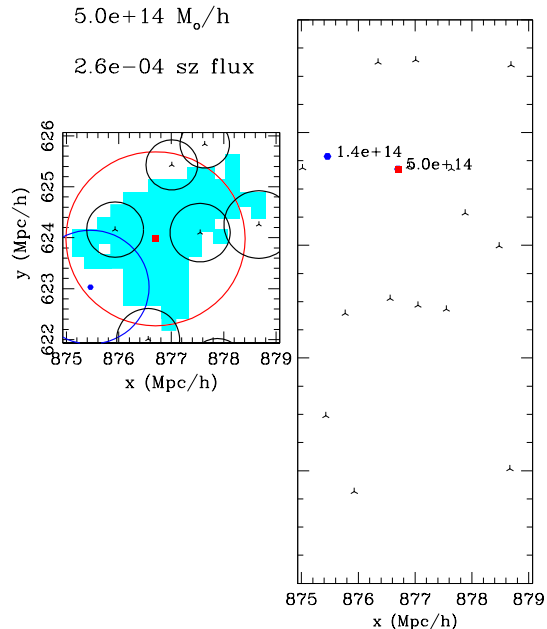


Figure 4. The left square is the SZ flux patch seen on the sky, and the filled solid square is the center of the most massive halo identified with this patch, corresponding to the cluster shown in Fig. 1. The filled dot at left is another $M \geq 10^{14} h^{-1} M_\odot$ halo near the SZ cluster, and the little “T” symbols are centers of $M \geq 10^{13} h^{-1} M_\odot$ halos in the region. Circles are taken to be $1 h^{-1} \text{Mpc}$ for the $10^{14} h^{-1} M_\odot$ halo, and scaled by $M^{1/3}$ for other masses. At right, the long axis is in the redshift direction and goes the entire $1000 h^{-1} \text{Mpc}$ of the box, and shows the halo positions in this direction (indicating masses of $\geq 10^{14} h^{-1} M_\odot$ halos).

or other properties. Finally we have optimistically assumed that foregrounds can be efficiently removed, perhaps by multi-frequency observation. With these caveats however we see that the SZ effect provides a very good means of catching all clusters. It also catches anything else that is hot enough along the line of sight between $z \sim 10^3$ and $z \simeq 0$.

Using SZ flux alone does not give redshifts for the found halos – although a method to estimate rough redshifts has been proposed (Schaefer, Frommer & Zaroubi 2005). Without redshifts one can still, for example, measure angular clustering and counts of galaxy clusters for cosmological parameters (e.g. Diaferio et al 2003; Mei & Bartlett 2003, 2004; Cohn & Kadota 2005) but this has much less information than the 3-dimensional counterparts (e.g. Viana & Liddle (1996, 1999); Haiman, Mohr and Holder (2001); Holder, Haiman and Mohr (2001); Carlstrom, Holder & Reese (2002); Levine, Schulz & White (2002(@); Weller, Battye & Kneissl (2002); Battye & Weller (2003); Weller & Battye (2003); Majumdar & Mohr (2004); Mohr (2005), see the review by Weller & Battye (2003) for more detailed references).

5 CATALOGUE COMBINATIONS

Given the three catalogues, each of which has objects with some measure of their mass, comparisons and combinations

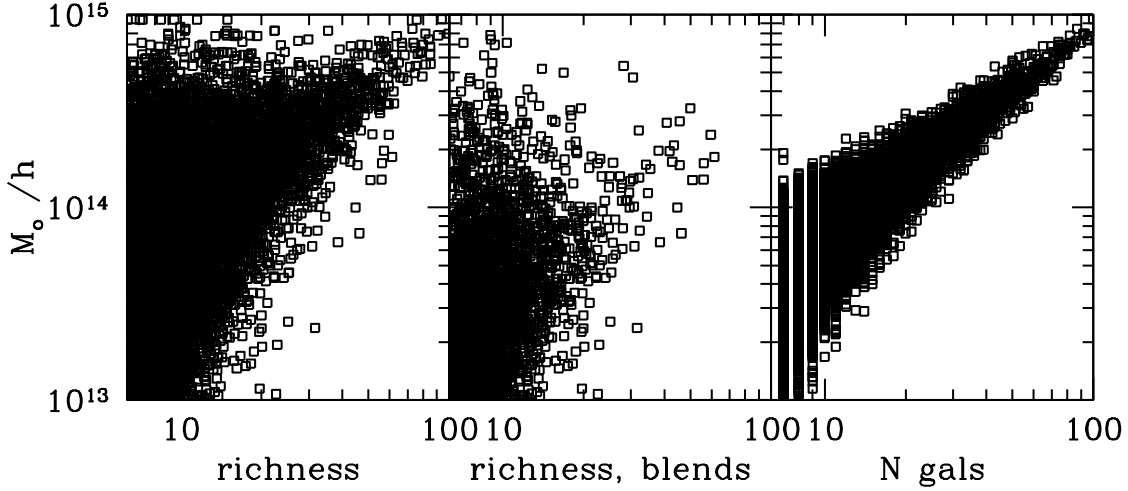


Figure 3. Left: the $\lg(\text{richness})$ - $\lg(\text{mass})$ relation for found clusters for the fiducial model described in the text. Center: the $\lg(\text{richness})$ - $\lg(\text{mass})$ relation for blends, those clusters with less than half their richness coming from galaxies belonging to any one dark matter halo. Right: the number of galaxies-mass relation for the dark matter halos. The scatter for the found clusters is 0.30 in $\lg(\text{mass})$, for those with richness ≥ 10 , while for the halos it is 0.13 in $\lg(\text{mass})$.

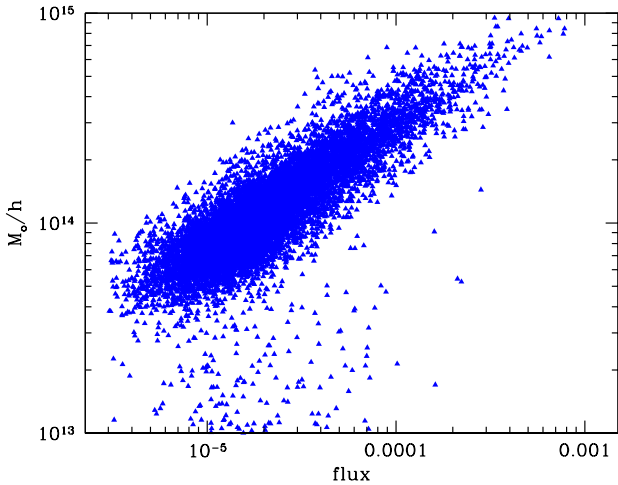


Figure 5. Mass for found SZ clusters at $z = 0.5$ as a function of SZ flux ($\mu K \text{ sr}$ or $0.23 T_{CMB} \text{ arcmin}^2$).

can now be made. Most matchings tend to be many to one – for example each dark matter halo can be matched to multiple optical or SZ clusters. We took each catalogue and found the best match in the other two catalogues for each object. For the dark matter halos the added information is the SZ patch with the most flux and the richest optical cluster. The results of this matching, in particular, the numbers of missed and overcounted halos, were reported above. The SZ cluster finder is much better at having at least one match for any massive halo in its catalogue, compared to the optical finder. (The $z = 0.5$ optical finder finds 2 of the 36 halos missed by

the fiducial SZ finder, the fiducial SZ finder finds 193 of the 227 missed by the optical finder.)

To associate found optical and SZ clusters to each other directly, without going through dark matter halos, we used a direct analogue of the assignment of halos to SZ patches. This procedure could also be used with observational data, where the true dark matter halos are not known. All optically found clusters with centers within 2 or fewer pixels of the SZ patch are assigned to the SZ patch (or cluster). The optical match of the SZ cluster is the richest of these optical clusters. If an optical cluster matches to more than one SZ cluster, it is assigned the SZ cluster with the largest flux. Generalizations of this are clear, but for simplicity we started with only one match per optical or SZ cluster, so that every optically found cluster gets an SZ flux (which might be zero) and every SZ found cluster gets an optical richness (which again might be zero). This matching does not require the corresponding optical and SZ halos to agree. For all optical clusters with richness ≥ 10 and non-zero SZ flux, $\sim 8\%$ of the optical and SZ halos differ in the fiducial case, with only a slight increase in catalogues with lower Δ_p .

To get a more complete combined SZ and optical catalogue it is useful to start with an optical catalogue which finds more massive halos than the fiducial optical catalogue does. The latter misses 15% of the most massive halos when optimized on its own. The idea is that an optical catalogue with more blends (lower Δ_p) can be combined with SZ information to cut out many these additional blends, ultimately producing a catalogue with more of the massive halos. As will be seen below, this does indeed work well in our simulations.

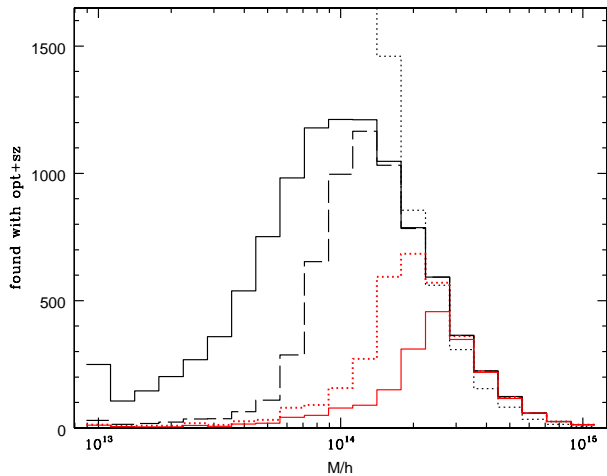


Figure 6. Number of massive halos found in the optical catalogue, requiring flux $\Delta T \geq (0, 1, 3, 5) \times 10^{-5} \mu\text{K sr}$ or $\Delta T \geq 0, 4.3, 13, 21 \times 10^{-5} T_{\text{CMB}} \text{arcmin}^2$, from left to right (solid, dashed, dotted, solid). The far left (solid) line is the mass distribution of the optical clusters with richness ≥ 10 without any SZ cut, requiring the cluster to have nonzero SZ flux gives a line very close to the dashed line, second from left. The high and lighter dotted line is the true number of massive halos, overcounted by the finders at the high mass end. A threshold on SZ flux is extremely good at weeding out low mass optical clusters.

5.1 Optical Catalogue Plus SZ Flux

The augmented optical catalogue is taken to include all optical clusters with richness ≥ 10 and a new requirement of SZ integrated flux above some cut:¹⁰ $\Delta T \geq 0, 1, 3, 5 \times 10^{-5} \mu\text{K sr}$ or $\Delta T \geq 0, 4.3, 13, 21 \times 10^{-5} T_{\text{CMB}} \text{arcmin}^2$ – for observations at frequency $\nu \ll 56.84 \text{ GHz}$ this corresponds to an integrated Y parameter smaller by a factor of 2. The number of massive halos found, as a function of mass and these cuts, is shown in Fig. 6.

For the three SZ cuts, the three rightmost solid lines in Fig. 6, the blend fraction goes down 25% from the fiducial optical case, even though the optical catalogue alone has a relaxed overdensity cut. The $\lg(\text{richness})-\lg(M)$ scatter goes down by 33%. The overcounting increases, running from 24%-20% from left to right. The three cuts using SZ flux differ in the number of massive halos missed. From left to right the number missed is down from the fiducial optical case by 40%, then is only slightly fewer and for the strongest cut misses almost twice as many.

5.2 SZ Catalog Plus Optical Richness

In the previous section, each optical cluster was assigned an SZ flux using the optical-SZ matching described above. One can instead start with an SZ catalogue and add optical information, to obtain an enhanced SZ catalogue. (These are not identical because the optical-SZ cluster matching is not one to one.) In this case we take the SZ catalogue with a cut of $3 \times 10^{-5} \mu\text{K sr}$, second from right in Fig. 6: the

number of missed halos is very slightly (from 15% to 16%) larger than in the fiducial optical catalogue, but the blends and scatter in the $\lg(\text{richness})-\lg(\text{mass})$ relation go down by a factor of 2, the scatter in the $\lg(\text{SZ flux})-\lg(\text{mass})$ relation goes up by 30% and the overcounting goes down by 20%. If overcounting is a concern, it is far better to start with the SZ catalogue and add optical richness information.

5.3 Outliers

With observational data, one only has the optical and SZ cluster catalogues, and not the underlying halo catalogues. One question which arises is how well the catalogues could be used together to flag outliers in the richness- or flux-mass relations, i.e. clusters which have an incorrect mass assignment. The optical and SZ scatter of the “true” halo mass from that predicted by the $\lg(\text{flux})-\lg(\text{mass})$ or $\lg(\text{richness})-\lg(\text{mass})$ relation are $\sim 50\%-70\%$ correlated, depending upon how the catalogues are chosen. This is not surprising as both SZ flux and galaxy richness suffer from projection effects, so the scatter in mass is due in part to the same source. Even with this correlation, however, outliers can be reduced to some extent.

Fig. 7 shows where found clusters fall on the SZ and optical mass relation if they are assigned both – in this case we are taking the true mass to be the mass of the best matched optical halo for both the SZ and optical finders. At left are those clusters ($\sim 90\%$) which are $\leq 2\sigma$ of the $\lg(\text{richness})-\lg(\text{flux})-\lg(\text{mass})$ relation, at right are those further away from the mean relations. Slightly over half of these $> 2\sigma$ outliers in predicted to true mass are clusters which have their SZ best matched halo not agreeing with their optical best matched halo, and this is true of all of the $> 5\sigma$ outliers. A discouraging trend to notice is that there are many clusters whose SZ and optical predicted masses agree very well, which might lend confidence to their values, but whose true masses are actually lying far off (sometimes $> 5\sigma$) of this relation. However, one can also take this relation and find the mean relation ($\lg(\text{flux})$ as a function of $\lg(\text{richness})$ or vice versa) and cut out objects which lie more than 1σ off of it. It appears most promising (Fig. 8) to use SZ predicted mass as a function of optical predicted mass and cut 1σ optical outliers on this relation – these clusters seem more likely to be true outliers in their predicted mass as a function of optical richness.

There is also a small correlation with number of optical clusters in an SZ patch and the size of the scatter of the SZ or its best matched optical cluster’s mass from the mean relation¹¹ as can be seen in Fig. 9. That is, SZ clusters with more optical cluster matches are more likely to be off of the mean $\lg(\text{flux})$ or $\lg(\text{richness})-\lg(\text{mass})$ relation.

6 JOINT SZ-OPTICAL CLUSTER FINDING

Instead of finding clusters separately using galaxy and SZ flux maps and then combining catalogues one can use the optical and SZ information concurrently to find clusters. We

¹⁰ The peak must also be above $4\sigma_{\text{noise}}$.

¹¹ We thank A. Leauthaud for suggesting we plot this quantity.

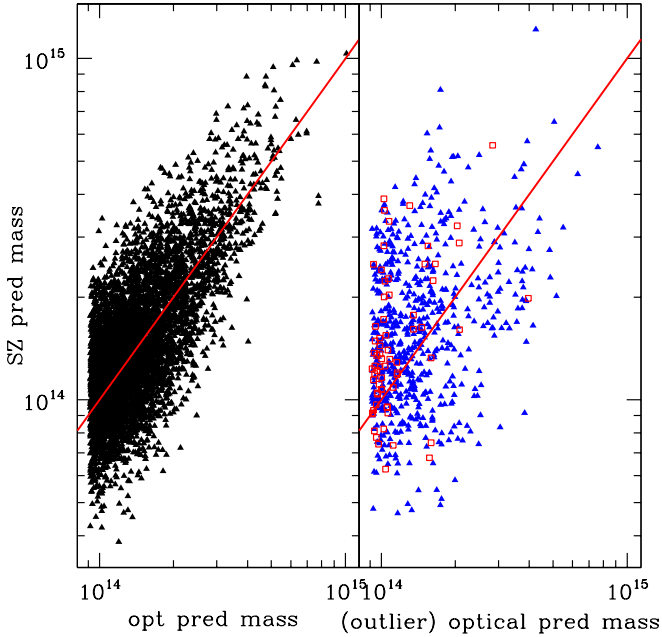


Figure 7. Predicted mass using optical “richness” (x-axis) and SZ flux (y-axis) for clusters which are within 2σ of the mean $\lg(\text{flux})$ - or $\lg(\text{richness})$ - $\lg(\text{mass})$ relation for both SZ and optical (left figure) or above 2 (triangles) or 5σ (squares) for either (right figure). The halo mass, compared to the predicted optical or SZ mass, is taken to be that corresponding to the optical cluster.

investigated a number of simple ways of doing this joint cluster finding.

A straightforward generalization of the optical finder is to start with the SZ peak catalogue and then use each peak as a potential center for optical cluster finding. The optical finding is identical to that above (centered on a given luminous galaxy) except that there is no a priori redshift for the candidate cluster center. Instead, the finder scans through 50 different redshift bins, each of width $20 h^{-1} \text{Mpc}$, and keeps the cluster with the most richness for each SZ peak. Again the overdensity Δ_p is tuned to the most massive halos, calibrated in this case for the most massive halos in the dark matter simulation using an offset of the diagonal length across a pixel ($\sim 0.35 h^{-1} \text{Mpc}$) as the SZ peak position can be anywhere within the pixel.

This joint finding is a marked improvement compared to the cases above (optical alone, or merging separate SZ and optical catalogues). Although the number of missed massive halos remains about the same, the number of blends goes down by almost a factor of 2, the $\lg(\text{richness})$ - $\lg(\text{mass})$ scatter goes down by $> 40\%$, the $\lg(\text{flux})$ - $\lg(\text{mass})$ scatter is about the same, and the overcounting goes down from a factor of 20% to 2%. Essentially, by using the SZ peak as a way to find cluster centers, one is more likely to start near a cluster center.

Two extensions were explored as well. As many halos were “lost” because they weren’t the dominant halo in an SZ patch, one can use the SZ patch as an indicator of hot gas and then search for not one, but many clusters within each SZ patch. After finding the first SZ peak-centered optical cluster, we sorted the remaining galaxies in order of

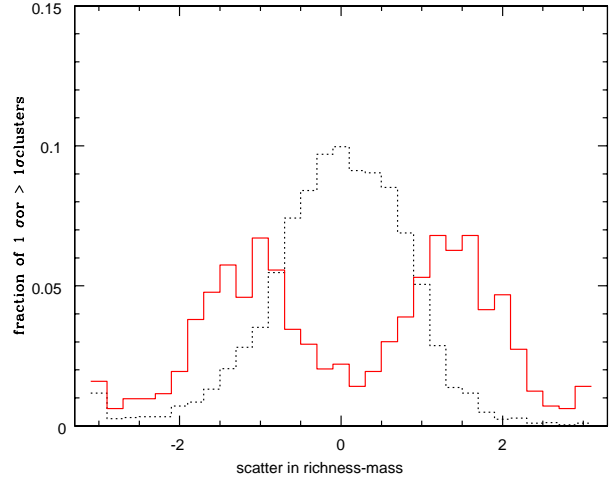


Figure 8. Scatter off of optical $\lg(\text{richness})$ - $\lg(\text{mass})$ relation for clusters which are within 1σ of the optical-SZ predicted mass relation in Fig. 7 above (dotted line) and those which are $\geq 1\sigma$ off (solid line). This suggests that making a 1σ cut on clusters using the optical-mass vs. SZ mass relation will tend to cut out clusters which are outliers in the $\lg(\text{richness})$ - $\lg(\text{mass})$ relation.

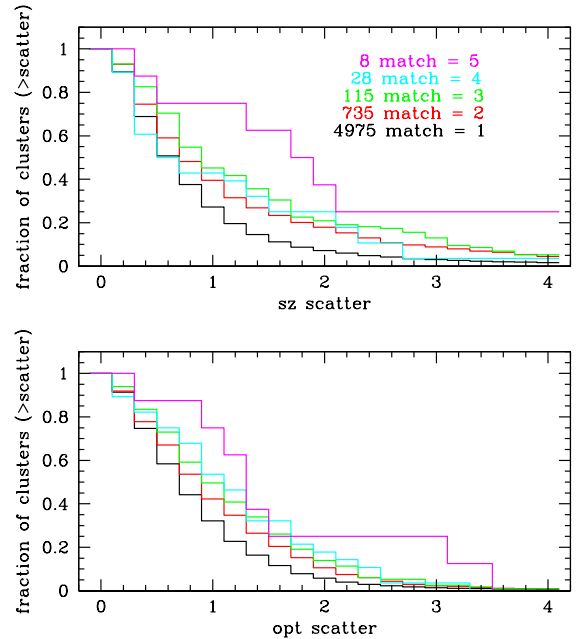


Figure 9. The fraction of clusters with scatter above a certain amount in units of the width σ of the mean $\lg(\text{flux})$ or $\lg(\text{richness})$ - $\lg(\text{mass})$ relation). SZ clusters with more optical cluster matches tend to have a larger scatter off of the mean relation, both for the SZ predicted mass and the optical predicted mass. The lines go from most to fewest matches of optical to SZ patches, essentially from top to bottom, in each picture.

decreasing luminosity and repeated the usual optical cluster finding. One finds that the more such clusters one includes (e.g. keeping up to 3 of the clusters in each peak), the fewer rich halos are missed. However, the success with respect to the rest of the criteria worsen, compared to the 1 optical cluster per SZ peak case above: blends, scatters and overcounting all increase.

A second generalization is to start instead with the unmerged SZ flux maps. In this case, one is using all the local SZ peaks as cluster finding centers, even if the peak is in a patch that adjoins another, rather than just the largest peak in the contiguous region. Doing this for the SZ cluster finding alone increases the $\lg(\text{flux})-\lg(\text{mass})$ scatter by 40%, and results in an overcounting by almost twice the number of massive halos in the box (80%, ~ 6 times higher than the unmerged SZ cluster finder). However, using unmerged SZ peaks as a starting point for optical cluster finding allows the optical cluster search to cut down the overcounting. For this case (one cluster per unmerged SZ peak), the number of halos compared to the fiducial optical case which are missed goes down by $\sim 33\%$, the blends go down by $\sim 33\%$, the overcounting barely decreases and the scatter in $\lg(\text{richness})-\lg(\text{mass})$ goes down by $\sim 33\%$. The scatter in $\lg(\text{flux})-\lg(\text{mass})$ goes up by $\sim 30\%$.

7 GENERAL TRENDS

Generally, combining optical and SZ catalogues works substantially better on all fronts than either individually – as hoped – and the joint finding offers further improvements. The tradeoff between decreasing blends and increasing completeness can be seen in Fig. 10, as a function of changing overdensity cut Δ_p . To summarize the different methods shown:

- Optical alone (light dotted lines at left): the fiducial optical model.
- Optical + SZ (dashed lines): using an SZ catalogue and optical catalogue together, keeping all SZ clusters which have a matching optical cluster. The optical catalogue has a relaxed (lower) overdensity threshold compared to the fiducial optical catalogue, to be more complete (it correspondingly has more blends on its own than the fiducial optical catalogue).
- SZ centered optical (solid lines): for each SZ peak, search for an optical cluster using the SZ peak as the center position, taking the redshift to be that for the center which gives the richest cluster.
- SZ + many optical (heavy dot-dashed): for each SZ peak, search for an optical cluster using the SZ peak as the center, as above, then continue to look for more optical clusters using the rest of the galaxies in the SZ patch as possible centers, in order of decreasing luminosity. Moving along the line includes more and more of these other optical clusters in the same patch, in the order they were found.
- SZ centered, no merging (heavy dotted): in the SZ finding, instead of merging all SZ clusters whose regions touch into one cluster, with one main peak, take each unmerged peak as a separate possible optical cluster center and search around it.

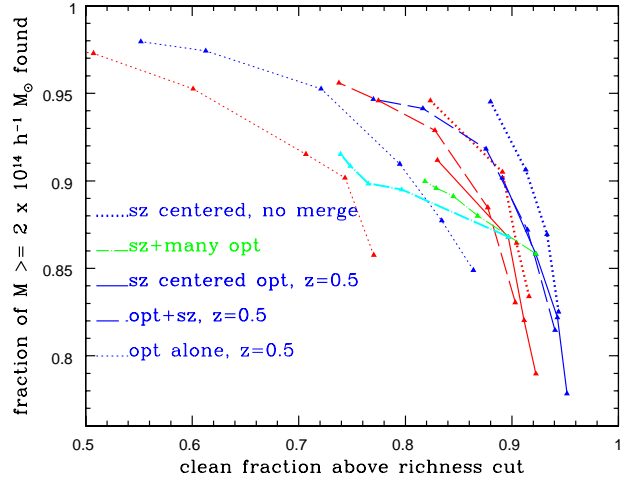


Figure 10. A comparison of clean fractions and completeness for several different cluster finders. The best finders are towards the upper righthand corner, having a high clean fraction and a high fraction of found massive halos. The light solid dotted lines (upper $z = 0.5$, lower $z = 0.9$) correspond to the optical search alone, changing Δ_p . Increasing Δ_p increases the clean fraction, but decreases the fraction of massive halos found. The dashed lines are the combined SZ and optical catalogues, the solid lines are optical searches around SZ cluster peaks and the heavy dotted lines are optical searches around SZ cluster peaks where the SZ cluster map does not merge adjoining clusters, again all for variation of the optical overdensity parameter. Also shown are the results where optical clusters are searched for in SZ clusters starting with a search around the central SZ peak position and then continuing to look for other optical clusters within the same SZ cluster. In this case, the number of additional clusters changes along the line, starting with 1 and then increasing. As more clusters per patch are included, more halos are found, but many of them are blends; the clean fraction decreases.

In all cases, the upper line in a given pattern is for $z = 0.5$; the combined finders all work better at lower redshift. Ideally the cluster finders would give results far to the right (large clean fraction) and far upwards (large fraction found), but the tradeoff between clean fraction and fraction found (or purity vs. completeness) is evident in the trajectories for each method.

From this diagram, one sees that the most clean clusters are obtained by using either optical cluster finding around SZ cluster peaks (merged or unmerged) or using one optical cluster match to each SZ peak by taking an SZ catalogue and matching one optical cluster to each SZ cluster. However these are not all equivalent in terms of the other criteria, the numbers for which are listed in Tables 1 and Tables 2. In particular, although the scatters are similar for all three, the (merged) SZ centered optical search has much less overcounting than the other two methods. (Recall this overcounting is not with respect to the number of uniquely found massive halos but with respect to the total number of massive halos. To get the former requires multiplying by the total number of massive halos divided by the number of uniquely found halos.) For $z \sim 0.9$, the optical finder is worse and alone gives slightly more overcounting relative to $z \sim 0.5$ for the same Δ_p cuts. When SZ is brought in (except

method	blend fraction (finding 90% massive)	scatter lg(richness)-lg(mass)	scatter lg(flux)-lg(mass)	overcounting
optical only	19%	≥ 0.30	–	17%-33%
SZ catalogue + optical catalogue	11%	0.18-0.19	0.12	14%-17%
SZ peak centered optical search	11%	0.17-0.18	0.10-0.11	1%-3%
SZ peak centered without merging	8%	0.19	0.12-0.13	11%-23%
SZ peak centered many optical	18%	0.18-0.29	0.11-0.31	2%-5%
SZ alone (merged)	–	–	0.10	13%
SZ alone (unmerged)	–	–	0.14	75%

Table 1. Properties of finders for redshift $z \sim 0.5$: blend fraction when 90% of massive halos are found, interpolated from Fig. 10, as well as properties not shown there: scatter in $\lg(\text{richness})-\lg(\text{mass})$, $\lg(\text{flux})-\lg(\text{mass})$, and overcounting. The latter is the number of massive halos found divided by the total number of massive halos present.

for the no merging case) the overcounting drops slightly, the SZ scatter is smaller and the optical scatter drops as well. The optical cluster finder is expected to do worse at high redshift because of the increased number of mergers (which are difficult to find in the plane of the sky using a circular overdensity finder, reducing the number of found halos) and the increase in relative number of possible interlopers per high mass halo (as the latter decreases much more sharply than the former with increasing redshift). The high mass halos are also more biased at high redshift.

Different cutoffs in richness or SZ-flux can be used in the blend fraction measurement compared to the completeness measurement to take into account the presence of scatter in these observables with mass. Some of these options are discussed in the appendix of Cohn et al (2007). We thank the referee for suggesting we mention this point.

7.1 Redshifts

One of the reasons for obtaining optical information for an SZ catalogue is to get redshifts. The redshifts we assign are based on galaxy redshifts, which themselves have a 2% photo- z scatter in our simulations, so some scatter is expected between the measured redshift (that of the central galaxy) and the true halo redshift even for clusters found by optical searches alone. The fraction of optical clusters whose redshift distance separation from their halo exceeds a certain amount is shown in Fig. 11, at left. As the box is periodic, separations are $< 500 h^{-1}\text{Mpc}$. The scatter is similar to (but slightly smaller than) that expected for a Gaussian separation distribution corresponding to distances for 2% photo- z errors ($\sigma = 71 h^{-1}\text{Mpc}$), also shown. The scatter between measured and true redshift is not only due to photo- z scatter, since an optical cluster can match to a different halo than that of the central galaxy, as mentioned earlier. However, as can be seen, the actual scatter at large separations is smaller than the Gaussian prediction, likely

because the cluster finder selects against objects with too large separations.

The corresponding redshift errors for the SZ clusters, either those given redshifts by finding associated clusters in an optical catalogue (§5.2) or by doing optical searching around SZ peaks (§6) are shown in Fig. 11. For the former case, we restrict to the 86% of the SZ clusters whose optical counterpart is centered within $0.5 h^{-1}\text{Mpc}$ of the peak in the plane of the sky (as otherwise it might be expected that the SZ peak and optical cluster would be flagged as corresponding to different objects). The true redshift is taken to be that of the most massive halo in the SZ patch (the SZ halo), the measured redshift is either that of the central galaxy of the matched optical cluster (for catalogue matching) or the redshift slice for the SZ peak centered optical search. In both, we see a tail to large separations not found in the optical case alone. This is due to the optical clusters whose best matched halo is not the same as the SZ matched halo ($\sim 3\%$ of the time for the SZ clusters matched to the most massive halos). In addition, for the SZ centered optical searches, for separations between $50\text{-}150 h^{-1}\text{Mpc}$ the scatter is lower than the random scatter expected from a 2% photo- z scatter of the center galaxy. In this case, the redshift is taken to be the redshift which has the most galaxy richness centered on it, rather than that of a specific (scattered) galaxy. As the galaxies are scattered independently, finding the central redshift of the clump of galaxies is a closer approximation to the true halo redshift than the redshift of the central galaxy.¹² This leads to no improvement if the optical (albeit SZ centered) cluster halo does not match the SZ halo, again leading to a large separation tail for a small fraction of the clusters.

¹² In principle this could also be used to find an improved redshift of the clusters that are centered on optical galaxies.

method	blend fraction (finding 90% massive)	scatter lg(richness)-lg(mass)	scatter lg(flux)-lg(mass)	overcounting
optical only	25%	≥ 0.34	–	15%-29%
SZ catalogue + optical catalogue	13%	0.19-0.20	0.11-0.12	16%-20%
SZ peak centered optical search	15%	0.17-0.18	0.10	1%-4%
SZ peak centered without merging	10%	0.18	0.12-0.13	12%-27%
SZ peak centered many optical	24%	0.17-0.34	0.10-0.34	2%-11%
SZ alone (merged)	–	–	0.10	17%
SZ alone (unmerged)	–	–	0.13	87%

Table 2. Properties of finders for redshift $z \sim 0.9$, as in Table 1 for redshift $z \sim 0.5$.

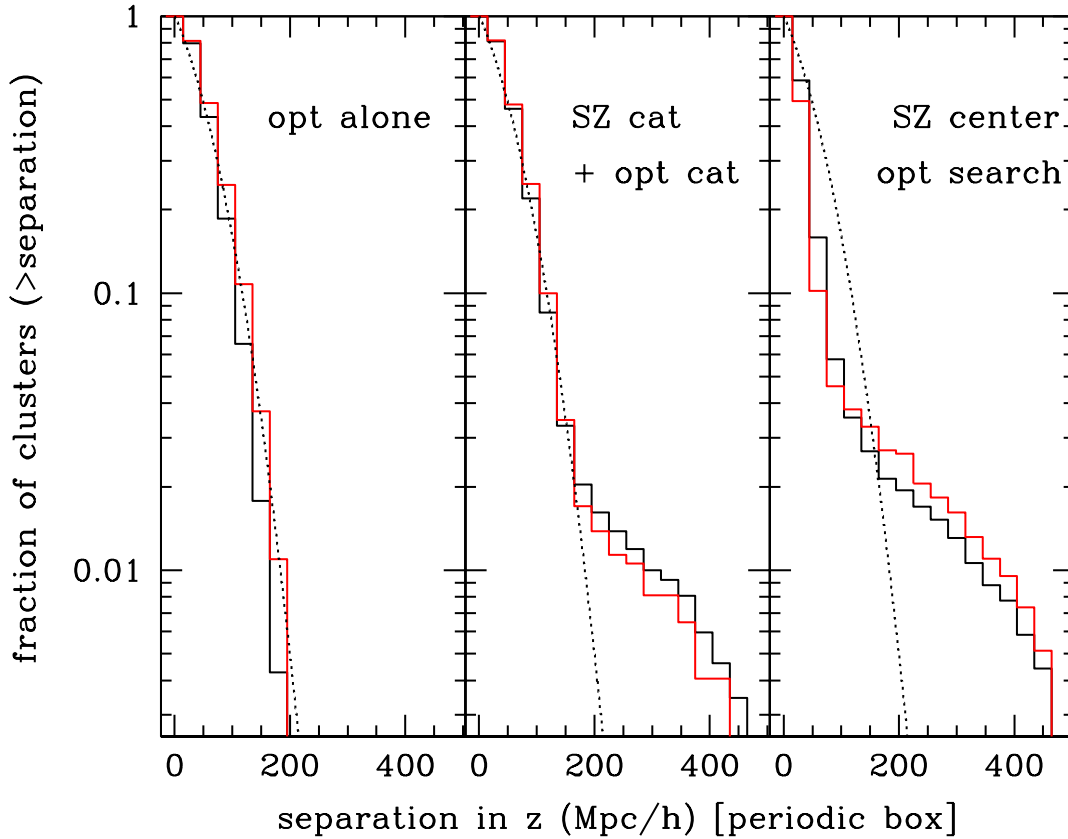


Figure 11. Cumulative fraction of SZ clusters above a given separation (measured position vs. halo true position in redshift direction) for (left) optically found clusters, (middle) SZ clusters matched to optical clusters, (right) optical clusters found around SZ peaks. For the latter two, the true halo is taken to be the SZ halo (the most massive halo in the SZ patch). The measured position is taken to be the redshift of the central galaxy for clusters centered on galaxies, and the redshift slice found by the optical search for the cluster centered on an SZ peak. The dotted line is the cumulative fraction of objects with Gaussian separations corresponding to $\sim 2\%$ photo- z errors ($\sigma = 71 h^{-1} \text{Mpc}$). The upper line at low separations for left and central, and at high ($\sim > 150 h^{-1} \text{Mpc}$) separations for left and right, corresponds to halos with mass $\geq 2 \times 10^{14} h^{-1} M_{\odot}$.

8 DISCUSSION AND SUMMARY

Using mock galaxy catalogs and SZ flux maps made from the $z = 0.5$ and 0.9 outputs of a $1 h^{-1}\text{Gpc}$ dark matter simulation, we have made a preliminary investigation of improvements in galaxy cluster finding that arise when optical and SZ surveys are combined. Our errors, beam, etc. were guided by expected properties for the DES and SPT experiments, though they are quite similar to other experiments in progress or soon to begin. We suggested a set of criteria by which to judge cluster finders and showed the corresponding tradeoffs which arose in some simple cases. Catalogues were compared using the number of massive ($\geq 2 \times 10^{14} h^{-1} M_{\odot}$) halos found, the fraction of clusters whose galaxy content was dominated by one underlying halo, the scatter in the $\lg(\text{richness})$ - or $\lg(\text{flux})$ - $\lg(\text{mass})$ relation and the overcounting of massive halos.

As hoped, using two catalogues jointly or using optical cluster finding centered on SZ flux peaks both led to great improvements in the catalogues. When using the two catalogues together to catch more high mass halos, it was preferable to take a more complete optical catalogue, (but more noisy, i.e. including more blends) and let SZ flux cuts weed out some of the outliers. Using SZ peaks as centers for optical searches and using 1 SZ peak per optical cluster worked similarly in terms of blends and finding massive halos, but worked much better in terms of overcounting. Using a relaxed (i.e. not merged) SZ catalogue for centering the optical search did well for some criteria but led to a large amount of overcounting.

In the combined catalogues we have two estimates of the cluster mass. Since the scatters in the richness- and flux-mass relations are correlated (both arising in part from projection effects) equality of the two estimates did not indicate a correct assignment of mass. However, taking out $> 1\sigma$ outliers in SZ mass predictions as a function of optical mass predictions did cut out many of the optical outliers (i.e. optical clusters whose predicted mass is $> 2\sigma$ from the true mass). There was a trend of SZ patches which had more optical clusters within them to be more likely to have their (optical or SZ) predicted and true mass differ.

We also compared the redshift of the found optical cluster to that of the best match halo to the SZ patch. The redshift was closer if the optical cluster was centered on the SZ peak, but even in the optical case alone there was a scatter due to the photo- z scatter of the central galaxy, and from the best match halo not being the same as the halo of the central galaxy giving the cluster redshift. Except for completeness, the trends were similar at both redshifts. At high redshift, the SZ effect was more effective at finding the massive halos and the optical finder was worse. Similarly, the optical finder worked better in a $\sigma_8 = 0.9$ catalogue than in the ones used here, more evidence for trends of FoF vs. SO finders with cosmology discussed in Lukic et al (2008).

These promising results are expected, for the most part, to generalize to more sophisticated finders and catalogues. Our mock catalogs were deliberately designed to be simple, having periodic edges and no light-cone evolution. The catalogues underestimate the projection effects, as only those within the box are included and do not include catastrophic photo- z failures. In addition it was assumed that the flux map could be perfectly cleaned of foregrounds, and scatter

in flux as a function of mass (due to e.g., cluster history or hydrodynamical effects such as shocks) is not included¹³.

Correspondingly, our simple cluster finders did not take full advantage of the properties of clusters or cluster galaxies, and could certainly be improved. There are many extensions possible to the simple finders used here. A review of optical cluster finders can be found in Gal (2006), and SZ cluster finders are improving as well (e.g. Schulz & White 2003; Delabrouille et al 2002; Geisbuesch, Kneissl & Hobson 2005; Pierpaoli and Anthoine 2005; Pierpaoli et al 2005; Pires et al 2005; Schaefer et al 2006a,b; Melin, Bartlett & Delabrouille 2006). In particular, using profile information (such as used in matched filters, e.g. Postman et al 1996; White & Kochanek 2002; Kochanek et al 2003; Dong et al 2007), changing the way halos are assigned to SZ peaks, using the peak size, etc., can all refine the cluster information. One extreme, if one is only interested in cluster finding as a route to cosmological parameters, would be to bypass the cluster finding entirely and just cross-correlate the SZ flux and galaxy maps, and compare to mock catalog predictions for the cross-correlation.

Several issues we raised for the simple finders will become more pressing with more sophisticated finders – cluster finders with increased complexity depend more and more upon the expected properties of the targets. In particular, finders can succeed or fail in several different ways and choices must be made about which failures/successes one cares most about. Specifically, as finders will be increasingly tuned and trained on mock catalogues, and no finder will be perfect, the question arises as to which errors are preferable. Ideally the errors should not only be as small as possible, but also well modeled in the mock catalogues. It is preferable to have a finder which relies most heavily upon the most accurate features of the mock catalogues at hand. This is especially important as the finders become more complex and assumed cluster properties become more and more implicit. In addition, there is a question of how the scatter in the finders depends on the target cluster masses, for example higher mass lowers the importance of shot noise errors on the optical richness and is more likely to correspond to a significant SZ signal. Our focus was on massive ($\geq 2 \times 10^{14} h^{-1} M_{\odot}$) halos, as the SZ methods cannot probe to very low masses, but the particular science goals may argue for a different threshold. The tradeoffs chosen in creating the finder should in part be decided by the intended use of the sample. Usually, the more complex the finder becomes the more tradeoffs are necessary in desirable catalogue features. These decisions are best made with an eye the strengths, features and science goals of the particular observational data set in hand, and the strengths of the mock catalogues available to analyze the data. As such multi-method cluster observations increase, the exciting science within reach will also increase dramatically.

JDC thanks C. Heymans, J. Kollmeier, A. Leauthaud, A. Meiksin, R. Nichol, P. Norberg, W. Percival, C. Pfrommer and E. Rozo for discussions. We would like to thank

¹³ A model to incorporate some of the effects of cluster history, especially merging, in the SZ signal in cosmological maps has been introduced by Bode et al. (2007); Shaw, Holder & Bode (2007).

U. Portsmouth, the ROE and IUCAA for hospitality and the opportunity to present this work while in progress and completed. We thank G. Evrard for comments on the draft and the anonymous referee for very helpful comments on the submitted paper. JDC acknowledges NSF-AST-0810820 and DOE for additional support. MW is supported by NASA and the DOE. The simulations used in this paper were performed and analyzed at the National Energy Research Scientific Computing Center.

Menanteau et al (2008) appeared when we were preparing this paper for publication, which discusses optical clusters found in the Southern Cosmology Survey and their expected SZ signal from ACT.

REFERENCES

- Abell, G.O., 1958, ApJS 3,211
- Arnaud M., Pointecouteau E., Pratt G.W., 2007, A&A 474L, 37
- Battye, R.A., Weller, J., 2003, PRD, 68, 083506
- Bode P., Ostriker J.P., Weller J., Shaw L., 2007, ApJ, 663, 139
- Bower, R., Lucey, J.R., & Ellis, R.S., 1992, MNRAS, 254, 601
- Brown, M.J.I., et al, 2008, ApJ to appear, arXiv/0804.2293
- Carlstrom, J.E., Holder, G.P., Reese, E.D., 2002, ARA&A, 40, 643
- Cohn J.D., Evrard A.E., White M., Croton D.J., Ellingson E., 2007, MNRAS, 382, 1738
- Cohn, J.D., Kadota, K., 2005, ApJ, 632, 1
- Dalton, G.B., Efstathiou, G., Maddox, S.J., & Sutherland, W.J., 1992, ApJL 390, L1
- Davis, M., Efstathiou, G., Frenk, C.S., White, S.D.M. 1985, ApJ, 292, 371
- Delabrouille, J., Melin, J.-B., Bartlett, J. G., 2002, ASPC proceedings, 257, 81
- Diaferio, A., Nusser, A., Yoshida, N., Sunyaev, R.A., 2003, MNRAS, 338, 322
- Dong, F., Pierpaoli, E., Gunn, J.E., Wechsler, R.H., 2007, ApJ to appear, preprint[arXiv:0709.0759]
- Evrard, A.E. et al, 2008, ApJ, 672, 122
- Gal R.R., 2006, preprint[arxiv:astro-ph/0601195]
- Gal, R. R., Lubin, L. M., Squires, G. K., 2005, AJ, 129, 1827
- Geisbuesch, J., Kneissl, R., Hobson, M., 2005, MNRAS, 360, 41
- Gerke B., et al., 2005, ApJ, 625, 6
- Gladders, M.D., Yee, H.K.C., 2000, AJ 120, 2148, see also <http://www.astro.utoronto.ca/~gladders/RCS/>
- Gladders, M.D., Yee, H.K.C., 2005, ApJS 157, 1
- Gladders, M.D., et al, 2007, ApJ 655, 128
- Haiman, Z., Mohr, J.J., Holder, G.P., 2001, ApJ, 553, 545
- Hallman, E.J., O'Shea, B.W., Burns, J.O., Norman, M.L., Harkness, R., Wagner, R., 2007, ApJ 671, 27
- Heitmann, K., et al, 2008, Computational Science and Discovery, in press [arXiv:0706.1270]
- Holder, G., Haiman, Z., Mohr, J.J., 2001, ApJL, 560, 111
- Holder, G.P., McCarthy, I.G., Babul, A., 2007, MNRAS 382, 1697
- Jannuzi, B. T., & Dey, A., 1999, in ASP Conf. Ser. 191: Photometric Redshifts and the Detection of High Redshift Galaxies, ed. R. Weymann, L. Storrie-Lombardi, M. Sawicki, & R. Brunner, 111
- Kochanek C.S., White M., Huchra J., Macri L., Jarrett T.H., Schneider S.E., Mader J., 2003, ApJ, 585, 161
- Levine, E. S., Schulz, A.E., White, M., 2002, ApJ, 577, 569
- Lopez-Cruz, O., 1997, PhD thesis, University of Toronto
- Lopez-Cruz, O., Barkhouse, W.A., Yee, H.K.C., 2004, ApJ 614, 679
- Lukic, Z., Reed, D., Habib, S., Heitmann, K, preprint arXiv:0803.3624
- Lumsden, S.L., Nichol, R.C., Collins, C.A., Guzzo, L., 1992, MNRAS 258,1
- Majumdar, S., Mohr, J.J., 2004, ApJ, 613, 41
- Mei, S., Bartlett, J.G., 2003, A&A, 410,767
- Mei, S., Bartlett, J.G., 2004, A&A, 425,1
- Melin, J.-B., Bartlett, J. G., Delabrouille, J., 2006, A&A, 459, 341
- Menanteau, F., Hughes, J.P., Jimenez, R., Hernandez-Monteagudo, C., Verde, L., Kosowsky, A., Moodley, K., Roche, N., 2008, arXiv:0808.0214
- Miller, C.J., et al, 2005, AJ, 130, 968
- Mohr, J.J., 2005, in ASP Conf. Ser. 339: Observing Dark Energy, ed. S.C. Wolf & T.R. Lauer, 140-151
- Pierpaoli, E., Anthoine, S., 2005, AdSpR, 36, 75
- Pierpaoli, E., Anthoine, S., Huffenberger, K., Daubechies, I., 2005, MNRAS, 359, 261
- Pires, S., Juin, J.B., Yvon, D., Moudden, Y., Anthoine, S., Pierpaoli, E., 2005, A&A, 455, 741
- Postman M., Lubin L.M., Gunn J.E., Oke J.B., Hoessel J.G., Schneider D.P., Christensen J.A., 1996, AJ, 111, 615
- Ross N.P., et al., 2007, MNRAS, 381, 573
- Ruhl, J., et al, 2004, SPIE, 5498, 11
- Schulz A., White M., 2003, ApJ 586, 723
- Schaefer, B.M., Pfrommer, C., Zaroubi, S., 2005, MNRAS, 362, 1418
- Schaefer, B.M., Pfrommer, C., Hell, R., Bartelmann, M., 2006, MNRAS, 370, 1713
- Schaefer, B.M., Pfrommer, C., Bartelmann, M., Springel, V., 2006, MNRAS, 370, 1309
- Shaw, L.D., Holder, G.P., Bode, P., 2007, arXiv0710.4555S
- Sunyaev R. A. & Zel'dovich, 1972, Comm. Astrophys, Space Phy., 4, 173
- Sunyaev R. A. & Zel'dovich, Ya. B., 1980, ARA&A, 18, 537
- Tinker, J.L., Kravtsov, A.V., Klypin, A., Abazajian, K., Warren, M.S., Yepes, G., Gottloeber, S., Holz, D.E., 2008, preprint arXiv:0803.2706
- Vale C., White M., 2006, New Astronomy, 11, 207
- Viana, P. T. P., Liddle, A.R., 1996, MNRAS, 281, 323
- Viana, P. T. P., Liddle, A.R., 1999, MNRAS, 303, 535
- Voit, G.M., 2005, RMP, 77, 207
- Weller, J., Battye, R.A., Kneissl, R., 2002, PRL, 88, 1301
- Weller, J., Battye, R.A., 2003, NewAR, 47, 775
- White, R., et al 1999, AJ 118, 2014
- White, M., 2002, ApJs, 579, 16
- White M., Hernquist L., Springel V., 2002, ApJ 579, 16
- White M., Kochanek C.S., 2002, ApJ, 574, 24
- White M., Zheng Z., Brown M. J. I., Dey A., Jannuzi, B. T. 2007, ApJ, 655, 69
- Wilson G., Muzzin A., Lacy M., Yee H., Surace J., Lonsdale C., Hoekstra H., Majumdar S., Gilbank D. & Gladders M. ("the SpARCS Collaboration"), 2006, conference pro-

ceedings “Spitzer Space Telescope: Infrared Diagnostics of Galaxy Evolution”, ed. Chary, R.